Ionics (2023) 29:2021–2029
https://doi.org/10.1007/s11581-023-04944-w

ORIGINAL PAPER

Electrochemical biosensor based on antibody-modified Au nanoparticles for rapid and sensitive analysis of influenza A virus

Qiwen Bao[1] · Gang Li[1] · Zhengchun Yang[2] · Jun Liu[2] · Hanjie Wang[3] · Gaoju Pang[3] · Qianjin Guo[4] · Jun Wei[5] · Wenbo Cheng[6] · Ling Lin[1]

Received: 11 December 2022 / Revised: 27 February 2023 / Accepted: 2 March 2023 / Published online: 9 March 2023

Abstract

To cope with the easy transmissibility of the avian influenza A virus subtype H1N1, a biosensor was developed for rapid and highly sensitive electrochemical immunoassay. Based on the principle of specific binding between antibody and virus molecules, the active molecule-antibody-adapter structure was formed on the surface of an Au NP substrate electrode; it included a highly specific surface area and good electrochemical activity for selective amplification detection of the H1N1 virus. The electrochemical test results showed that the BSA/H1N1 Ab/Glu/Cys/Au NPs/CP electrode was used for the electrochemical detection of the H1N1 virus with a sensitivity of 92.1 μA $(pg/mL)^{-1}$ cm^2, LOD of 0.25 pg/ml, linear ranges of 0.25–5 pg/mL, and linearity of ($R^2 = 0.9846$). A convenient H1N1 antibody-based electrochemical electrode for the molecular detection of the H1N1 virus will be of great use in the field of epidemic prevention and raw poultry protection.

Keywords Au NPs · H1N1 virus · Virus sensor · Immunoassay

Introduction

The avian form of the influenza A virus subtype H1N1 spreads widely and causes great harm. Its transmission is not limited to birds and poultry; its mutated strain can also infect humans, where the probability of death from the virus is high. The H1N1 virus is spread by body contact and droplets, causing respiratory illness in patients with symptoms similar to those of a common cold, such as coughing and fever [1]. Currently, there are many methods used to detect influenza viruses, such as polymerase chain reaction (PCR) [2], enzyme-linked immunosorbent assay (ELISA) [3], viral plaque assay [4], reverse transcription loop-mediated isothermal amplification assay [5–7], and viral flow cytometry [8]. These traditional virus testing methods are accurate and reliable, but most of them involve complex sample processing, expensive equipment, consumable materials, and professional operating technicians. These drawbacks limit their application to portable, in-line analysis scenarios. For example, when Shahsavandi et al. [9] used the rHA 10 ELISA method for the detection of the H9 subtype influenza virus, they needed to titrate the antibody onto 96 polystyrene plates and then measure the optical density value at 450 nm using an automatic plate spectrophotometer; in addition, they needed to design multiple control experiments. Furthermore, PCR technology is difficult to apply to the

✉ Ling Lin
linling@tju.edu.cn

1 School of Precision Instrument and Optoelectronic Engineering, the State Key Laboratory of Precision Measuring Technology and Instruments, Tianjin University, 92 Weijin Road, Tianjin 300072, China

2 School of Electrical and Electronic Engineering, Tianjin Key Laboratory of Film Electronic & Communication Devices, Advanced Materials and Printed Electronics Center, Tianjin University of Technology, Tianjin 300384, China

3 School of Life Sciences, Tianjin Engineering Center of Micro-Nano Biomaterials and Detection-Treatment Technology, Tianjin Key Laboratory of Function and Application of Biological Macromolecular Structures, Tianjin University, 92 Weijin Road, Tianjin 300072, China

4 Analysis and Testing Center, Tianjin University, 92 Weijin Road, Tianjin 300072, China

5 School of Materials Science and Engineering, Harbin Institute of Technology, Shenzhen 518055, China

6 Suzhou Institute of Biomedical Engineering and Technology, Chinese Academy of Sciences, Suzhou 215163, People's Republic of China

field and real-time virus analysis because it requires expensive instruments and complex processing and testing methods [10]. It can be found that it is important to adopt a cheaper and more convenient testing technique, especially for use in developing countries, such as electrochemical methods [11–13].

Electrochemical immunoassay is widely used in the field of virus diagnosis, and it has advantages such as the following: simple technique and low manufacturing cost. In recent years, researchers have been focused on the development of electrochemical equipment with excellent performance and portability that can be used for on-site detection [14]. Researchers have proposed work that combines virus detection with portable electrochemical devices. For example, Laura et al. [15] developed an intelligent immune sensor, which combined a screen-printed electrode and a PalmSenS3 for the highly sensitive and reliable online detection of SARS-CoV-2. Many manufacturers can provide desktop or industrial electrochemical workstations all over the world, and more and more researchers are focusing their work on new detection methods and preparing new materials with higher performance. Nanomaterials have good physical, chemical, and biological properties, including small particle size, as well as a highly specific surface area, which provides more reaction sites for electrochemical reactions [16]. Therefore, many new nanomaterials have been developed and applied to biological immune sensors, such as graphene [17], polymer nanomaterials [18], dendrimers [19], conducting polymers [20], metal oxide nanomaterials [21], and nanomaterials [22]. Au NPs, as with other noble metal NPs, have many unique properties, such as simple preparation methods, large specific surface area, higher chemical and biological stability, and good biocompatibility [23]. In particular, Au NPs have good biocompatibility properties that make them widely used in clinical and medical research fields. Bin et al. [24] constructed a sandwich-structure quenched electrochemiluminescence immune sensor based on SnO_2/rGO/Au NPs for the detection of insulin and achieved high sensitivity, selectivity, and repeatability in the experiment. Pei et al. [25] prepared an electrochemical immunosensor for the quantitative detection of hepatitis B surface antigen using Au NPs loaded onto polypyrrole nanosheets as a platform and an Rh nucleus and Pt shell loaded onto amino-functionalized graphene nanosheets as markers. Nanomaterials are widely used in biological immunosensors because they can be used as enzyme carriers or signal markers of redox reaction reporters and electrode active substances [26–28].

Materials and methods

Materials and reagents

The $HAuCl_4{\cdot}3H_2O$, KNO_3, cysteamine hydrochloride (Cys), glutaric dialdehyde (Glu), bovine serum albumin (BSA), and sodium citrate were purchased from Shanghai Macklin Biochemical Co., Ltd. Recombinant Hemagglutinin-Influenza A Virus H1N1 California 04/2009 was purchased from Prospec-Tany TechnoGene Co., Ltd (Ness-Ziona, Israel). H1N1 Hemagglutinin 1 was purchased from Beijing Bioss Co., Ltd. Ethyl alcohol was purchased from Sigma-Aldrich, USA. The Ag/AgCl Carbon Paper (CP) and Pt electrodes were purchased from Tianjin Lanlike Chemical Electronic High Technology Co., LTD. Phosphate-buffered saline (PBS) was purchased from Sigma-Aldrich, USA.

Electrochemical measurements were conducted at an ambient temperature using a CHI 660E electrochemical workstation (CH Instruments, Inc., USA). Deionized water (~18.0 MΩ) was obtained from a Millipore system.

All synthetic materials and electrodes were characterized using the following tools: scanning electron microscopy (SEM) was performed using a Nova Nano SEM 430 scanning electron microscope.

Fabrication of Au NP/CP by thermal reduction

The CP (1 cm^2) surface was rinsed using 10 mL deionized water and alcohol successively to remove impurities from the surface, edges, and internal channels. Then, the clean CP electrode was placed in a vacuum-drying oven at 80 ℃ for 30 min. A total of 100 mL $HAuCl_4$ (0.01 wt%) was heated to a boil while stirring rapidly on an electromagnetic heater. Three milliliters of 1% sodium citrate was then quickly added along the glass bar to the boiling $HAuCl_4$ solution. We observed that the mixed solution gradually changed color from yellow to wine red upon stirring for 2 h. Then we transferred the sample solution to a clean sample bottle and sealed it. The reaction chemical formula was as follows:

$$Au^{3+} + Citrate \overset{Heat}{\rightarrow} Au^{+} + SADC \tag{1}$$

$$3Au^{+} - SADC \overset{Heat}{\rightarrow} 2Au^{0} + Au^{3+} \tag{2}$$

This reaction involved two processes: (1) Au^{3+} is rapidly reduced to Au^{+} by sodium citrate on the premise of sufficient sodium citrate; (2) the Au^{+} sodium pyruvate complex was self-disproportionated into Au^{0} and Au^{3+}, and pure Au NPs were obtained from the wine-red solution after the nucleation of gold atoms by high-speed centrifugation. We then added the high-concentration Au NP solution into a 1-mL sample tube and dropped high-purity water up to 0.5 mL. Finally, as shown in Step 1 of Fig. 1, a dispenser (SM200SX-3A, MUSASHI, Japan) was used to load the Au NP dispersion solution to draw a 1×1 cm^2 rectangular pattern in the central area of the CP electrode surface. During room-temperature drying, Au NPs were adsorbed onto the surface of the porous electrodes and into the internal channels.

Preparation of the H1N1 antibody and antigen

Because the H1N1 virus contains a variety of enzyme molecules, such as neuraminidase molecules and RNA polymerase, the preparation of the H1N1 virus solution needed to be carried out in the refrigerator at 4 ℃. In order to restore the original sample storage solution environment, 1 μg of provirus sample was mixed with 150 mM NaCl and 0.005% Tween-20 10 mM phosphoric acid, at a ratio of 1:10,000 and placed into 0.1 μg/mL of the virus solution; it was then stored in cold storage for future use. H1N1 Hemagglutinin 1 needs to be frozen in a −20°C freezer when not in use, and when preparing the H1N1 antibody solution we need, we quickly transfer it to a 4°C refrigerator freezer for operation. To obtain an undetermined 1 μg/mL antibody solution, we took 1 μL of 1 mg/mL antibody solution and mixed it with 0.01 M tris-buffered saline (pH 7.4) with 1% BSA, 0.03% Proclin300, and 50% glycerol at a ratio of 1:1000. Then, we quickly transferred the H1N1 antibody solution to the freezing chamber for storage.

Fabrication of BSA/H1N1 Ab/Glu/Cys/Au NP/CP electrodes

To create the sandwich-structured BSA/H1N1 Ab/Glu/Cys/Au NP/CP electrodes, we prepared the experimental environment and reagents beforehand. To create a moist water atmosphere environment, we cut a 1-cm-thick absorbent sponge with an area of 2×2 cm^2 and put it in a PBS kit filled with pH 7.0 for storage. It is well known that Cys is a core component of basic proteins in nature, and it has good electrochemical activity. Cys has a very active hydrogen-sulfur bond (-SH) in its molecular structure, which can easily form an Au-S covalent bond with Au and adsorb onto the surface of the Au electrode. At the same time, the terminal amino (-NH_2) group is free from the electrode, which can be used to rivet more active molecules. In our experiment, we took 1 mL of 10 mM Cys solution, prepared using PBS (pH 7.0), loaded it into the point hose, and shook it evenly. Then, the Au NP/CP (prepared in "Fabrication of Au NP/CP by thermal reduction") was tiled in the center of the sponge paper, and the process parameters of dispensing were set (at 9.8 kW), as shown in Step 2 of Fig. 1. A rectangular pattern covered with Au NPs was drawn in the 1×1 cm^2 central area and then quickly transferred to a cell incubator at 4 ℃ for incubation for 12 h. Pentanediol has two or more specific groups, including -NH_2, -HS, and -COOH, so it can be coupled to two or more molecules to statically bind them together. We used Glu here as an H1N1 antibody and Cys as a linking antibody for Au. The experimental steps were as follows: first, we removed the Cys/Au NP/CP electrodes incubated in the above steps, after which we placed them in PBS (pH 7.0) and gently rinsed them for 30 s. Then, a dispensing machine (at 9.8 kW) was used to load 1 mL of 2.5% pentanediol solution prepared using PBS (pH 7.0). A 1×1 cm^2 rectangular pattern was drawn on the central region of the Cys/Au NP/CP electrode and incubated for 12 h, as shown in Step 3 of Fig. 1. Then, 10 μL of 1 μg/mL antibody solution (prepared in "Preparation of the H1N1 antibody and antigen") was dropped onto the central region of the Glu/Cys/Au NP/CP electrode and placed on a sponge soaked with PBS (pH 7.4) for incubation for 1 h, as shown in Step 4

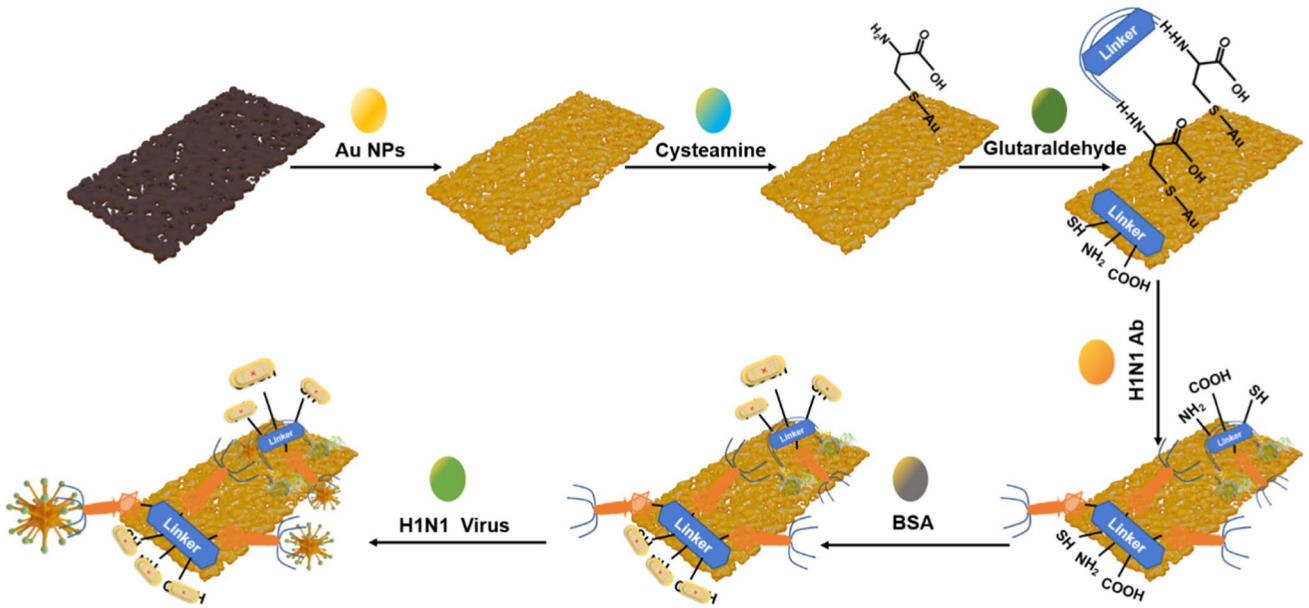

Fig. 1 Fabrication of the BSA/H1N1 Ab/Glu/Cys/Au NP/CP immunosensor

of Fig. 1. Then, the electrode surface was washed using PBS (pH 7.4), and 1 mL 1% BSA solution was added to block the non-specific binding sites on the electrode surface and Glu Linker and incubated for 30 min. Finally, PBS (pH 7.4) was used to wash off the excess BSA on the electrode surface, and the obtained BSA/H1N1 Ab/Glu/Cys/Au NP/CP electrodes were directly used for the next experiment or stored in a cold-storage room at a temperature of 4 ℃.

Results and discussion

Qualitative characterization

Au NPs performed XRD tests in the range of 20–90° to verify the composition of the prepared samples. By comparing the test results with XRD standard cards (Cubic, FM-3M (225), JCPDS No.04-0784), there are three obvious characteristic diffraction peaks of gold in (Fig. 2a, b), indicating that Au NPs were successfully prepared.

Carbon fibers are uniformly distributed with a diameter of about 10 μm (Fig. 3a). Furthermore, it can be clearly observed that many hollow structures are exposed on the randomly arranged carbon fiber structure, forming uniform active sites with an average diameter of about 25 μm. The corresponding elemental mappings (Fig. 3b, c) demonstrate the uniform distribution of C and Au in the Au NP/CP.

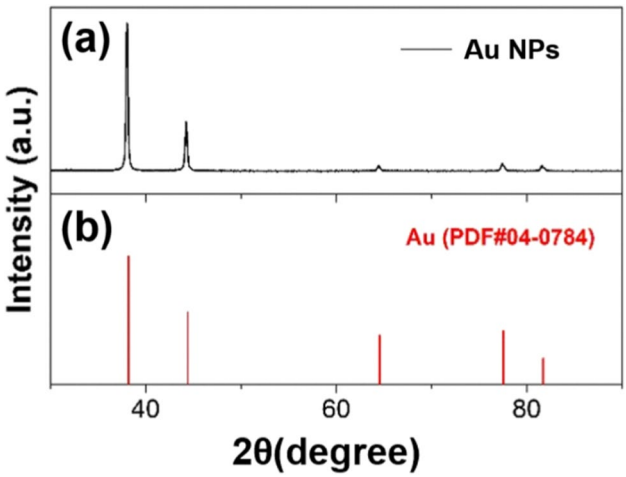

Fig. 2 XRD patterns of Au NPs

Electrochemical measurements

All the electrochemical experiments in this experiment were carried out in a CHI660E series electrochemical workstation. A 2×2 cm^2 Pt electrode, polished by alumina, was used as the counter electrode and the working electrode to form the current test loop. A very common commercial glass Ag/Ag Cl electrode was used as the reference electrode. The BSA/H1N1 Ab/Glu/Cys/Au NP/CP electrode prepared in this study was connected to the positive electrode of the potentiostat via a well-connected electrode column. The parameters of differential pulse voltammetry (DPV) in this paper were set as follows: voltage window range (−0.3–+0.3 V), amplitude (0.02 V), scan rate (50 mV/s), and sensitivity (10–4 A/V).

Testing principle of the immune sensor

The virus sample used in this experiment was the full-length glycosylated H1N1, model: California/04/2009, which possesses a recombinant hemagglutinin envelope protein produced using the baculovirus vector in insect cells, with a molecular weight (mW) of about 72 kDa. HA protein is the most important surface antigen of the virus, which is related to the virus adsorption through membranes and the infection of host cells. The amino spherical structure of the HA protein head can combine with aldehyde groups of different

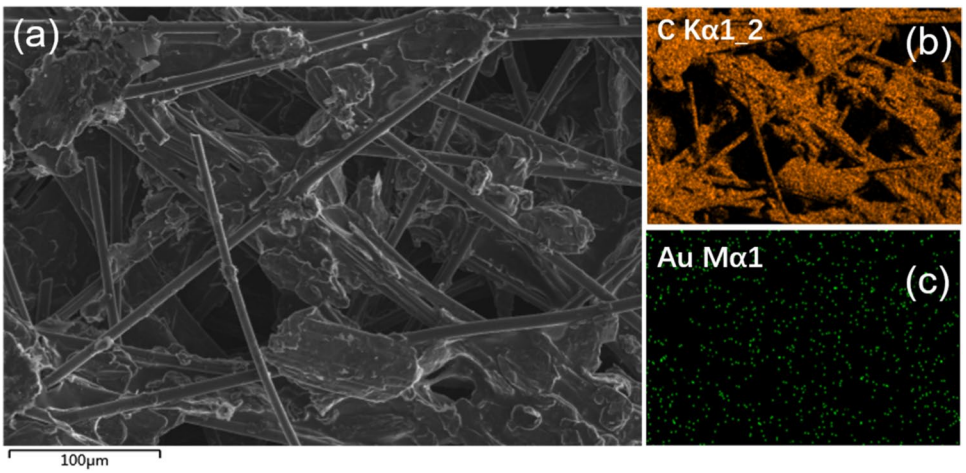

Fig. 3 **a** SEM image and **b**, **c** the image right are the distribution of C and Au element corresponding to **a**

receptors to form a stable collagen structure. To ensure the specific binding between the antigenic determinant cluster and the hypervariable region of the antibody molecule, as shown in Fig. 1, a layer of BSA solution was modified after the modification of the antibody to block the active sites on the electrode surface or Glu layer, to prevent them from occupying the reaction space of the antibody and antigen. The immune biosensor designed in this paper was based on the preemption of specific concentrations of antibodies fixed on the electrode surface or in the internal channels by antigens free from solution. In the experiment, every step of electrode operation, including the deposition of Au NPs onto the CP electrode, modification of Cys and Glu, immobilization of the antibody, and detection of different concentrations of the virus, was achieved using a REDOX+ peak current of H_2PO_4- and HPO_4-REDOX pairs in PBS. The antibody was bound to the active group on the Glu structure through the valence bond. Since the mW of the H1N1 antibody is about 72 kDa, when the antibody molecule covers the electrode surface, it blocks the REDOX current from reaching the electrode surface through the double electric layer of the electrode and solution, resulting in the reduction of the current signal. Based on this mechanism, we detected the current response caused by the combination of antigen and antibody by adding different concentrations of antigen into the solution to be tested and then analyzed the current-response antigen concentration DPV curve.

Electrochemical characterization of step modification of immunosensor

The BSA/H1N1 Ab/Glu/Cys/Au NP/CP composite electrode was obtained by layer modification on the hydrophilic CP electrode. To analyze the influence of each step of modification on the electrochemical performance of the electrode, their DPV curves were compared as shown in Fig. 4. Curve A is the DPV of the pure CP electrode in PBS, and it was found that no oxidation peak related to $H_2PO_4^-$ and HPO_4^- REDOX pairs in PBS appeared from −0.3 to +0.3 V. This phenomenon is related to the poor electrochemical activity of pure CP electrodes. After the deposition of Au NPs synthesized with the thermal reduction method, a cathodic reduction peak appears at −0.01 V, as shown in curve B. The overall current response density of curve B is about 1.2 times that of curve A. The significantly increased current response of Au NP/CP electrodes is attributed to the highly specific surface area, good biocompatibility, and excellent electron transfer capability of Au NPs. The current response of curve C is slightly lower than that of curve B, which may affect the electron transfer of the REDOX reaction with the amino group free from the Cys/Au NP/CP electrode in the solution. Curve D is the DPV of the electrode modified with Glu. It can be seen from the figure

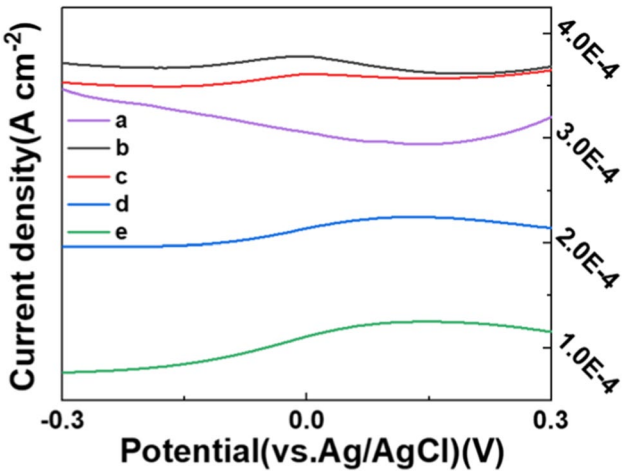

Fig. 4 Differential pulse voltammetry (DPV) curves recorded by the CP (**a**), Au NP/CP (**b**), Cys/Au NP/CP (**c**), Glu/Cys/Au NP/CP (**d**), and H1N1 Ab/Glu/Cys/Au NP/CP (**e**) in PBS (0.01 M)

that the current response of the Glu/Cys/Au NP/CP electrode is significantly reduced by about half compared with that of the Cys/Au NP/CP electrode. This is because Glu, as a small protein cross-linking agent, forms a rigid macromolecular structure by connecting its aldehyde group with the free amino group of the Cys/Au NP/CP electrode to prevent REDOX molecules from reaching the electrode surface. When the antibody was linked to the Glu cross-linker, the current response density of the composite electrode decreased further, by about half, as shown using line E. This also demonstrated that the antibody successfully modified the electrode surface. The decrease in current response may be related to the fact that the bulk protein structure formed via antibody curing on the electrode surface is not conducive to electron conduction between the double electric layers.

To analyze the effect of H1N1 Ab modification to the electrode surface on the electrochemical performance of the immunosensor electrode, we in PBS (0.01 M) containing 5 ng/ml H1N1 antigen studied the CV response of the electrode after each electrode modification step, and the comparative plots of the obtained CV curves are shown in Fig. 5. the parameters of the CV test were set as follows: scan speed (50 mV/s), and voltage interval (− 0.4–1.1 V). From Fig. 5, we can see that the upper and lower asymmetric CV curves indicate that no reversible electrochemical reaction occurs in the present electrochemical system of the composite electrode, and the absence of obvious oxidation and reduction peaks indicates that no redox reaction occurs in the system or the charge migration reaction rate on the electrode surface is much lower than the migration of reactant oxides from the native solution to the electrode surface and the migration of reductants generated by the reaction on the electrode surface to the native solution. rate. However, the current

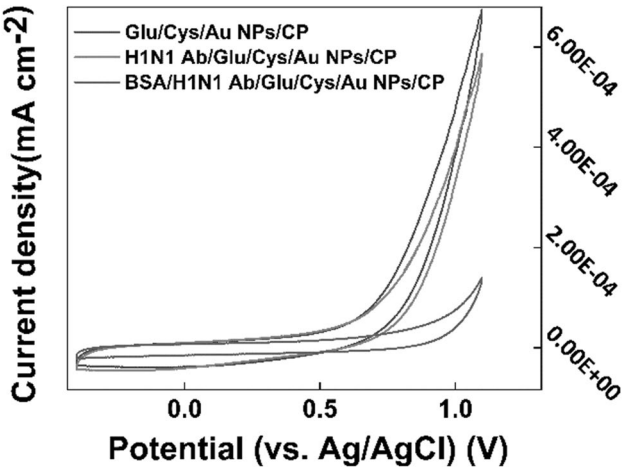

Fig. 5 Cycle voltammetry (CV) curves recorded by the Glu/Cys/Au NP/CP, H1N1 Ab/Glu/Cys/Au NP/CP and BSA/H1N1 Ab/Glu/Cys/Au NP/CP in PBS (0.01 M) containing 5 ng/ml H1N1 antigen

response of the CV curves of H1N1 Ab and BSA modified at the Glu/Cys/Au NP/CP electrode decreased significantly after the linear voltage was applied, which is also consistent with the conclusion that the decrease in current response may be related to the formation of large protein structures on the electrode surface by the solidification of antibodies or biomolecules, which does not facilitate the electron conduction between the bilayers. This is also consistent with the conclusion that the decrease in current response may be related to the fact that the large protein structure formed by the antibody or biomolecule solidified on the electrode surface is not conducive to the electron conduction between the bilayers.

Electrochemical properties of the modified electrode for the H1N1 antigen by an immunosensor

To compare the electrochemical responses of Au NP/CP, Cys/Au NP/CP, Glu/Cys/Au NP/CP, and H1N1 Ab/Glu/Cys/Au NP/CP to the H1N1 antigen (Fig. 6), we respectively tested their electrochemical responses in pure PBS. DPV in 0.25 and 5 pg/mL H1N1 antigen solution. To minimize systematic error during the experiment, all four electrodes were incubated under the same environmental conditions(incubation scene: cell incubator; temperature: 4 ℃; incubation time: 12h) and stored in the cold room at 4 ℃. To further minimize error, five of each electrode were prepared in the same way. Each electrode in each batch was tested in parallel in a specific concentration of H1N1 antigen solution, and the most representative DPV data were selected by comparing each dataset and eliminating those with large errors. As can be seen from Fig. 6a, b, both Au NP/CP and Cys/Au NP/CP have cathodic reduction peaks near −0.01 V. In addition, the two electrodes showed no significant electrochemical response to different concentrations of the H1N1 antigen. This conclusion is consistent with the absence of active sites on Au NPs' surfaces

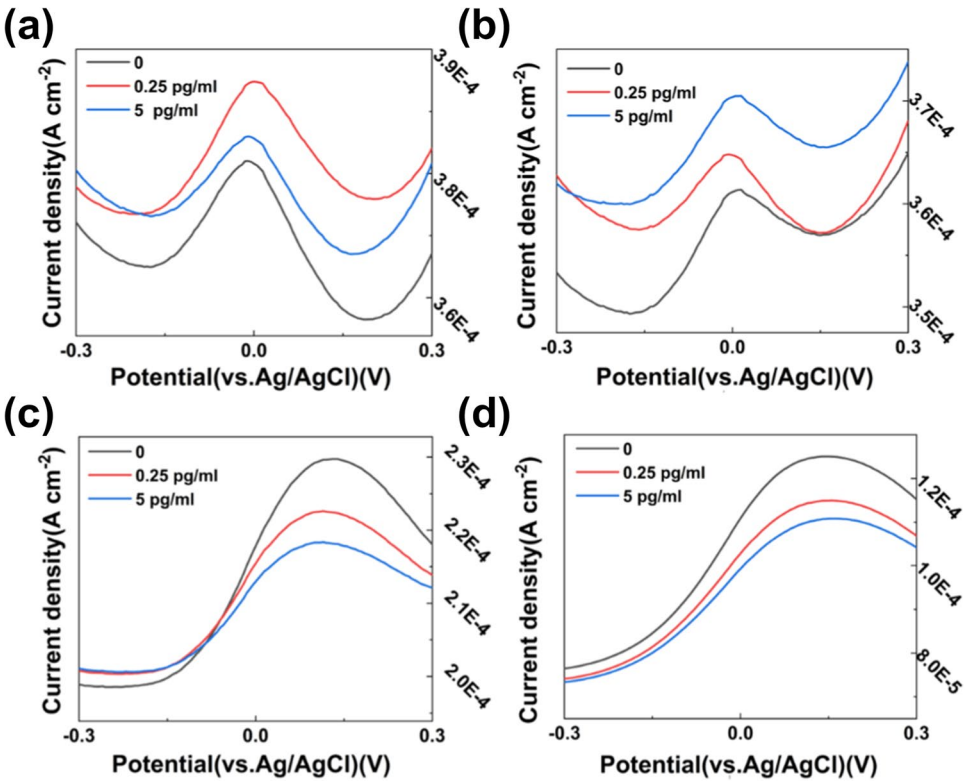

Fig. 6 DPV curve recorded by Au NP/CP, Cys/Au NP/CP, Glu/Cys/Au NP/CP, and H1N1 Ab/Glu/Cys/Au NP/CP DPV in PBS (0.01 M) containing 0, 0.25, and 5 pg/mL of H1N1 antigen, respectively

and the Cys molecular structure that can bind to the H1N1 antigen. As shown in Fig. 6c, d, after Glu, the H1N1 antibody was modified on the surface of the inactive Cys/Au NP/CP electrode, and the current response density of their DPV curves gradually decreased with the increased concentration of the H1N1 antigen in the solution. This experimental phenomenon also shows that in the presence of the H1N1 antigen in the solution environment, both Cys and the antibody can bind the antigen on the electrode surface to form a large protein molecular structure, resulting in the blocking effect of electron transport. In addition, we found that the H1N1 Ab/Glu/Cys/Au NP/CP electrode had more obvious blocking of REDOX electrons than the Glu/Cys/Au NP/CP electrode, which was also consistent with the conclusion in the "Electrochemical characterization of step modification of immunosensor" section. These results indicated that the H1N1 Ab/Glu/Cys/Au NP/CP electrode was specifically binding to the H1N1 antigen, in addition to the Glu structure that was not covered by the H1N1 antibody. This indicates that the synthesized sandwich structure of H1N1 Ab/Glu/Cys/Au NPs/CP electrode can further improve the detection performance of biosensors through signal amplification and specific recognition of signal reporter molecules and target molecules.

A histogram of peak current density and H1N1 antigen concentration of DPV data in each group in Fig. 7 was made (Fig. 6). As can be seen from Fig. 7a, the blocking effect of the Ab/Glu/Cys/Au NP/CP electrode on electron transmission is more obvious. Figure 7b shows the current-response antigen concentration histogram of the Ab/Glu/Cys/Au NP/CP and Glu/Cys/Au NP/CP electrodes in pure PBS and 0.25 pg/mL H1N1 antigen solution, respectively. What we found is that the current response density of the Glu/Cys/Au NP/CP electrode in 0.25 pg/mL H1N1 antigen solution decreased by 6.44×10^{-6} (A cm^{-2}), while the current density of the Ab/Glu/Cys/Au NP/CP electrode decreased by 10.12×10^{-6} (A cm^{-2}), which was about 1.6 times that of the Glu/Cys/Au NP/CP electrode. This indicates that for the Ab/Glu/Cys/Au NP/CP electrode in the solution containing the H1N1 antigen, the presence of the antibody causes more antigen to bind to the electrode surface, resulting in more electron blocking.

Electrochemical characteristics of BSA/Ab/Glu/Cys/Au NP/CP electrodes for H1N1 antigen detection

Before the composite electrode was used for H1N1 antigen detection, we modified the electrode using BSA based on the experiment in "Electrochemical properties of the modified electrode for the H1N1 antigen by an immunosensor". This was to block the active sites on the electrode surface that were unrelated to the antigen-antibody reaction to achieve specific detection. Figure 8a shows the DPV of the BSA/Ab/Glu/Cys/Au NP/CP composite electrode in 0.25–5 pg/mL H1N1 antigen solution. As can be seen from the figure, the current response of the same Ab/Glu/Cys/Au NP/CP electrode for continuous detection of different concentrations of the H1N1 antigen maintained good linearity in the range of 0.25–1.5 pg/mL. With the continuous addition of the H1N1 antigen, the current response of the negative electrode gradually reached saturation, where the signal slowly faded. This may be related to the limited number of antibodies modified on the electrode surface. When the H1N1 antigen is continuously added to the reaction zone, and when all the antibodies on the electrode surface bind to the H1N1 antigen, the excess antigen can no longer be found on the electrode to bind to the active site and can only be free in the solution. Figure 8b is the linear fitting curve of Fig. 8a. The electrochemical performance parameters of the BSA/Ab/Glu/Cys/Au NP/CP composite electrode for H1N1 antigen detection can be obtained as follows: A sensitivity of 92.1 μA $(pg/mL)^{-1}$ cm^2, LOD of 0.25 pg/mL, linear ranges of 0.25–5 pg/mL, and linearity of $R^2 = 0.9846$.

Table 1 shows the comparison results between the BSA/Ab/Glu/Cys/Au NP/CP composite electrode and the reported minimum detection limits of the biosensors. The results showed that the BSA/Ab/Glu/Cys/Au NP/CP composite electrode had a low detection limit for the H1N1 virus

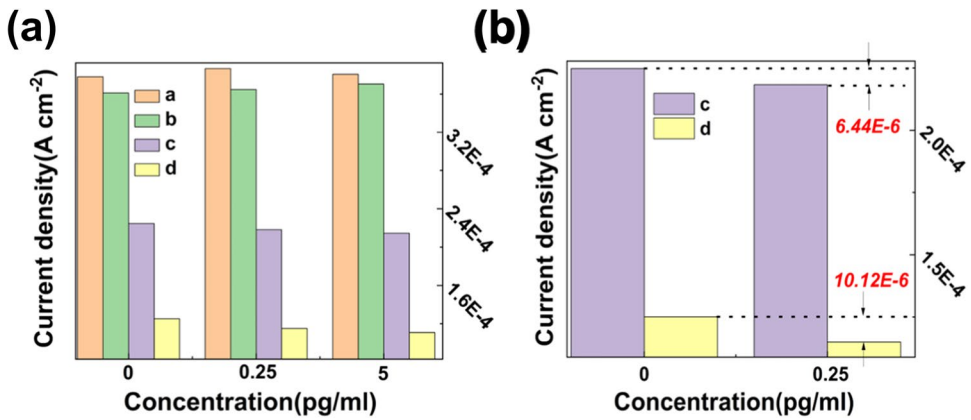

Fig. 7 Column diagram of CP (**a**), Au NP/CP (**b**), Cys/Au NP/CP (**c**), Glu/Cys/Au NP/CP (**d**), and H1N1 Ab/Glu/Cys/Au NP/CP (**e**) drawn according to the peak current response of the selected DPV line and the corresponding concentration

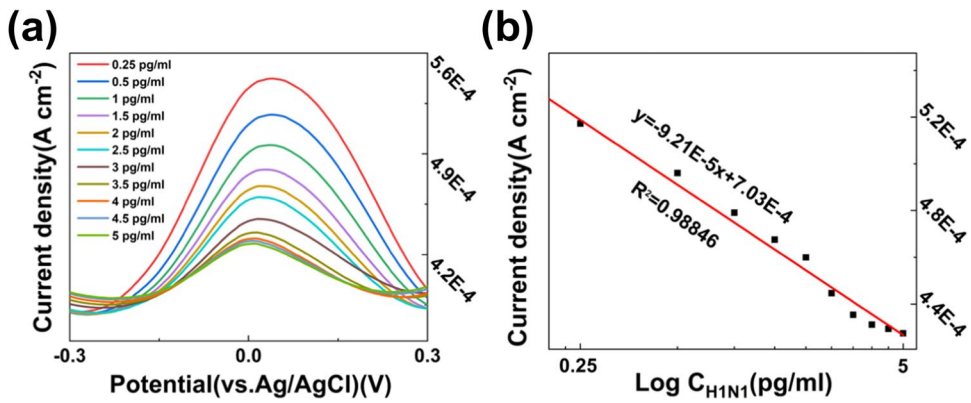

Fig. 8 **a** DPV curves obtained from BSA/H1N1 Ab/Glu/Cys/Au NP/CP composite electrode in the presence of PBS (0.01 M) containing 0–5 pg/mL of H1N1 antigen; **b** linear fitting curve

Table 1 Comparison of BSA/Ab/Glu/Cys/Au NPs/CP composite electrodes with the reported minimum detection limits for biosensors

Electrode	LOD	Substrate	*Antigen*	Ref
Anti-M1 ab/colloidal gold particles/Au electrode	20 pg/ml	Au electrode	M1 protein of H1N1 virus	[10]
Ab/RGO/CA/Au	0.5 PFU/ml	Au electrode	H1N1 influenza virus	[29]
α-2,6-sialyltransferase enzyme, α-2,3-sialyltransferase enzyme/Au/Si	0.05 μg/ml	Si electrode	HiN1	[30]
BSA/Ab/polyUiO-66@AgNPs/AE	0.0547 pg/ml	AE	H1N1 virus	[31]
Sialyloligosaccharide peptide/ BDD	3.3 PFU/ml	BDD	H1N1 virus	[32]
Ab-CH-CNT/C	113 PFU/ml	Carbon	H1N1 virus	[33]
Ab/Glu/Cys/Au NPs/CP	0.25 pg/ml	CP	H1N1 virus	This work

Conclusions

In this study, we present a low-cost, high-performance electrochemical immunosensor prepared by a dispensing process for the convenient detection of the H1N1 virus. The sandwich electrode was composed of hydrophilic CP, Au NPs, and antibodies for Glu and Cys. The electrode can be used for H1N1 virus detection only in PBS, which eliminates the tedious sample preparation process and has the potential to be used in a complex sample-testing environment. The biosensor showed high sensitivity (92.1 μA $(pg/mL)^{-1}$ cm^2), low detection limit (0.25 pg/mL), and good linearity (R^2 = 0.9846), and the test time was about 30 s. The results showed that this method has potential application value in the early diagnosis of H1N1 virus infection.

Supplementary Information The online version contains supplementary material available at https://doi.org/10.1007/s11581-023-04944-w.

Acknowledgements The authors would like to thank the State Key Laboratory of Precision Measuring Technology and Instruments for the use of their equipment. They are also thankful to Prof. Yang, Prof. Pan, and Ruizhao Tian from the Tianjin University of Technology for their guidance regarding experimental ideas and techniques as well as to Tianjin Guokeyigong Science and Technology Development Company for providing the access to the laboratory site and required equipment.

Funding This research was supported by the Tianjin Natural Science Foundation (Grant No. 18JCZDJC99800, 17JCQNJC00900), National Natural Science Foundation of China (Grant No. 51502203), Tianjin Young Overseas High-level Talent Plans (Grant No. 01001502), Tianjin Science and Technology Foundation (Grant No. 17ZXZNGX00090), Tianjin Distinguished Professor Foundation of Young Researchers, and Tianjin Development Program for Innovation and Entrepreneurship.

Declarations

Ethical statement The antigen and antibody experiments in this study do not involve biomedical research involving humans. All the procedures were performed in accordance with the Declaration of Helsinki and relevant policies in China.

Conflict of interest The authors declare no competing interests.

References

1. Lee DJ, Chander Y, Goyal SM, Cui TH (2011) Carbon nanotube electric immunoassay for the detection of swine influenza virus H1N1. Biosens Bioelectron 26(8):3482–3487
2. Templeton KE, Scheltinga SA, Beersma MFC, Kroes ACM, Claas ECJ (2004) Rapid and sensitive method using multiplex real-time PCR for diagnosis of infections by influenza A and influenza B viruses, respiratory syncytial virus, and parainfluenza viruses 1, 2, 3, and 4. J Clin Microbiol 42(4):1564–1569
3. Lee BW, Bey RF, Baarsch MJ, Simonson RR (1993) ELISA method for detection of influenza A infection in swine. J Vet Diagn Inv 5(4):510–515
4. Rameix-Welti MA, Munier S, Le Gal S, Cuvelier F, Agou F, Enouf V, Naffakh N, van der Werf S (2011) Neuraminidase of

2007–2008 influenza A(H1N1) viruses shows increased affinity for sialic acids due to the D344N substitution. Antivir Ther 16(4):597–603
5. Park G-S, Ku K, Baek S-H, Kim S-J, Kim SI, Kim B-T, Maeng J-S (2020) Development of reverse transcription loop-mediated isothermal amplification assays targeting severe acute respiratory syndrome coronavirus 2 (SARS-CoV-2). J Mol Diagn 22(6):729–735
6. Viet Loan Dao T, Herbst K, Boerner K, Meurer M, Kremer LPM, Kirrmaier D, Freistaedter A, Papagiannidis D, Galmozzi C, Stanifer ML, Boulant S, Klein S, Chlanda P, Khalid D, Miranda IB, Schnitzler P, Kraeusslich H-G, Knop M, Anders S (2020) A colorimetric RT-LAMP assay and LAMP-sequencing for detecting SARS-CoV-2 RNA in clinical samples. Sci Trans Med 12(556):eabc7075
7. Yan C, Cui J, Huang L, Du B, Chen L, Xue G, Li S, Zhang W, Zhao L, Sun Y, Yao H, Li N, Zhao H, Feng Y, Liu S, Zhang Q, Liu D, Yuan J (2020) Rapid and visual detection of 2019 novel coronavirus (SARS-CoV-2) by a reverse transcription loop-mediated isothermal amplification assay. Clin Microbiol Infect 26(6):773–779
8. Yeganeh B, Ghavami S, Rahim MN, Klonisch T, Halayko AJ, Coombs KM (2018) Autophagy activation is required for influenza A virus-induced apoptosis and replication. BBA-Mol Cell Res 1865(2):364–378
9. Shahsavandi S, Salmanian AH, Ghorashi SA, Masoudi S, Fotouhi F, Ebrahimi MM (2011) Development of rHA1-ELISA for specific and sensitive detection of H9 subtype influenza virus. J Virol Methods 171(1):260–263
10. Nidzworski D, Pranszke P, Grudniewska M, Krol E, Gromadzka B (2014) Universal biosensor for detection of influenza virus. Biosens Bioelectron 59:239–242
11. Liu ZQ, Tao JP, Zhu ZY, Zhang YL, Wang HB, Pang PF, Wang HB, Yang WR (2022) A sensitive electrochemical assay for T4 polynucleotide kinase activity based on Fe3O4@TiO2 and gold nanoparticles hybrid probe modified magnetic electrode. J Electrochem Soc 169(2):027504
12. Wang HB, Zhang HD, Xu LL, Gan T, Huang KJ, Liu YM (2014) Electrochemical biosensor for simultaneous determination of guanine and adenine based on dopamine-melanin colloidal nanospheres-graphene composites. J Solid State Electrochem 18(9):2435–2442
13. Wang HB, Zhang HD, Zhang YH, Chen H, Xu LL, Huang KJ, Liu YM (2015) Tungsten Disulfide nano-flowers/silver nanoparticles composites based electrochemical sensor for theophylline determination. J Electrochem Soc 162(7):B173–B179
14. Bao Q, Li G, Yang Z, Pan P, Liu J, Li R, Wei J, Hu W, Cheng W, Lin L (2021) In situ detection of heavy metal ions in sewage with screen-printed electrode-based portable electrochemical sensors. Analyst 146(18):5610–5618
15. Fabiani L, Saroglia M, Galata G, de Santis R, Fillo S, Luca V, Faggioni G, D'Amore N, Regalbuto E, Salvatori P, Terova G, Moscone D, Lista F, Arduini F (2021) Magnetic beads combined with carbon black -based screen-printed electrodes for COVID-19: a reliable and miniaturized electrochemical immunosensor for SARS-CoV-2 detection in saliva. Biosens Bioelectron 171:112686
16. Piscitelli A, Pennacchio A, Longobardi S, Velotta R, Giardina P (2017) Vmh2 hydrophobin as a tool for the development of "self-immobilizing" enzymes for biosensing. Biotechnol Bioeng 114(1):46–52
17. Adhikari BR, Govindhan M, Chen AC (2015) Sensitive detection of acetaminophen with graphene-based electrochemical sensor. Electrochim Acta 162:198–204
18. Duncan TV, Pillai K (2015) Release of engineered nanomaterials from polymer nanocomposites: diffusion, dissolution, and desorption. ACS Appl Mater Interfaces 7(1):2–19
19. Miodek A, Mejri N, Gomgnimbou M, Sola C, Korri-Youssoufi H (2015) E-DNA sensor of mycobacterium tuberculosis based on electrochemical assembly of nanomaterials (MWCNTs/PPy/PAMAM). Anal Chem 87(18):9257–9264
20. Wang JX, Wang MR, Guan J, Wang CY, Wang GX (2017) Construction of a non-enzymatic sensor based on the poly(o-phenylenediamine)/Ag-NPs composites for detecting glucose in blood. Mater Sci Eng C-Mater Biol Appl 71:844–851
21. Kannan P, Dolinska J, Maiyalagan T, Opallo M (2014) Facile and rapid synthesis of Pd nanodendrites for electrocatalysis and surface-enhanced Raman scattering applications. Nanoscale 6(19):11169–11176
22. Smith BR, Gambhir SS (2017) Nanomaterials for in vivo imaging. Chem Rev 117(3):901–986
23. Masitas RA, Allen SL, Zamborini FP (2016) Size-dependent electrophoretic deposition of catalytic gold nanoparticles. J Am Chem Soc 138(47):15295–15298
24. Xing B, Zhu WJ, Zheng XP, Zhu YY, Wei Q, Wu D (2018) Electrochemiluminescence immunosensor based on quenching effect of SiO2@PDA on SnO2/rGO/Au NPs-luminol for insulin detection. Sensors Actuators B-Chem 265:403–411
25. Pei FB, Wang P, Ma EH, Yang QS, Yu HX, Gao CX, Li YY, Liu Q, Dong YH (2019) A sandwich-type electrochemical immunosensor based on RhPt NDs/NH2-GS and Au NPs/PPy NS for quantitative detection hepatitis B surface antigen. Bioelectrochemistry 126:92–98
26. Ou LB, Xia N (2022) Progress in nanomaterials-based electrochemical biosensors for the detection of interleukins. Int J Electrochem Sci 17(4):220449
27. Xia N, Sun ZF, Ding FY, Wang YN, Sun WN, Liu L (2021) Protease biosensor by conversion of a homogeneous assay into a surface-tethered electrochemical analysis based on streptavidin-biotin interactions. Acs Sensors 6(3):1166–1173
28. Zhang YT, Chen F, Xie H, Zhou BB (2022) Electrochemical biosensors for the detection of SARS-CoV-2 pathogen and protein biomarkers. Int J Electrochem Sci 17(5):220541
29. Singh R, Hong S, Jang J (2017) Label-free detection of influenza viruses using a reduced graphene oxide-based electrochemical immunosensor integrated with a microfluidic platform. Sci Rep 7:42771
30. Wicklein B, del Burgo MAM, Yuste M, Carregal-Romero E, Llobera A, Darder M, Aranda P, Ortin J, del Real G, Fernandez-Sanchez C, Ruiz-Hitzky E (2013) Biomimetic architectures for the impedimetric discrimination of influenza virus phenotypes. Adv Func Mater 23(2):254–262
31. Jia QJ, Lou YF, Rong FL, Zhang S, Wang MH, He LH, Zhang ZH, Du M (2021) Silver nanoparticle embedded polymer-zirconium-based metal-organic framework (polyUiO-66) for electrochemical biosensors of respiratory viruses. J Mater Chem C 9(40):14190–14200
32. Matsubara T, Ujie M, Yamamoto T, Einaga Y, Daidoji T, Nakaya T, Sato T (2020) Avian Influenza virus detection by optimized peptide termination on a boron-doped diamond electrode. Acs Sensors 5(2):431–439
33. Devarakonda S, Singh R, Bhardwaj J, Jang J (2017) Cost-effective and handmade paper-based immunosensing device for electrochemical detection of influenza virus. Sensors 17(11):2597